Steering Control Improvement of Active Surgical Needle using Mosquito Proboscis-inspired Cannula

Sharad Raj Acharya
Department of Mechanical Engineering,
Temple University
Philadelphia, PA 19122
Sharad.acharya@temple.edu

Doyoung Kim
Department of Mechanical Engineering,
Temple University
Philadelphia, PA 19122
Doyoung.kim@temple.edu

Parsaoran Hutapea*
Professor, ASME Fellow
Department of Mechanical Engineering,
Temple University
Philadelphia, PA 19122
Parsaoran.hutapea@temple.edu

Abstract

Active needles have demonstrated superior tip deflection and improved accuracy compared to passive needles enhancing the efficacy of percutaneous needle insertion procedures. Successful navigation of these needles through tissues to reach targets relies on factors such as the actuation mechanism, tip shape, and surface geometry. In this study, we investigated the advantages of modifying the surface geometry of the active needle shaft, focusing on two improving crucial aspects: a) needle tip deflection and b) trajectory

* Corresponding author: Parsaoran.hutapea@temple.edu

tracking during tissue insertion. Prior research had shown that modifying the surface geometry of passive needles reduced friction force, tissue displacement, and tissue damage. Building on this knowledge and being motivated by the surface geometry of mosquito proboscis, our study proposed a bioinspired design modification on the active needle cannula. The active needle with the mosquito proboscis-inspired cannula was tested to measure the changes in insertion force, tip deflection, and trajectory tracking during polyvinyl chloride (PVC) phantom tissue insertions. Results showed that passive bevel-tip needles reduced insertion force by up to 10.67%. In active needles, tip deflection increased by 12.91% at 150mm insertion depth when the cannula was modified. The bioinspired cannula improved trajectory tracking error in the active needle by 39.00% while utilizing up to 17.65% lower control duty cycle. The enhancement of tip deflection and tracking control is expected to improve percutaneous procedures by achieving better patient outcomes and significantly mitigating the risk of complications.

Keywords: Mosquito Proboscis-inspired Cannula, Active Needle, Shape Memory Alloy (SMA), Insertion Force, Deflection, Tracking Error, Control.

1. Introduction

This study proposed a novel approach by introducing a mosquito proboscis-inspired cannula for active steerable needles to increase the needle tip deflection and reduce trajectory tracking errors during tissue insertion. The active needle with the modified cannula was designed for percutaneous procedures such as biopsy and brachytherapy to reach a desired target in soft tissues: liver, prostate, or kidney. An active needle can

generate large tip deflection and travel in a controlled path along a curved trajectory inside the tissues [1], which is considered a limitation in a conventional passive bevel tip needle. The passive bevel-tip needle deflects solely due to the unbalanced cutting force on its asymmetric tip. Additionally, as the needle travels into the tissue, the friction in the needle-tissue interface increases, and this deforms the tissue, undermining the needle placement accuracy and reducing the efficacy of the needle-based procedures. As a result, the uncertainties such as uncontrolled needle bending, and tissue deformation diminish the capability of the active needle to obtain accurate needle placement [2]. A tip-actuating active needle can compensate for the error caused by uncontrolled needle bending and tissue deformation [3] but does not have any means to minimize them. Thus, to minimize the uncertainties associated with the placement of active steerable needles and to facilitate desirable needle-tissue interaction, a mosquito proboscis-inspired design on the needle cannula was proposed in this study.

According to Ma et al. [4], bioinspired needles can be categorized based on five objectives: 1) minimizing insertion force, 2) reducing tissue deformation, 3) increasing the needle's maneuverability, 4) enhancing the needle's adhesion ability, and 5) other applications. We modified the active needle design with bioinspired features from a mosquito proboscis to achieve increased maneuverability. The mosquito proboscis-inspired feature would reduce the insertion force and tissue deformation leading to desirable large needle tip deflection and accurate trajectory tracking control. Needle insertion force consists of cutting force at the needle tip and friction force at the needle-tissue interface [5]. The needle insertion force is measured as the axial reaction force at the needle base during insertion. Several studies have been conducted on modifying needle tip geometry to reduce the cutting forces. In this

study, we designed the active needle with a conical tip (a symmetrical tip) to prevent the needle tip deflection in the absence of actuation. We studied the post-puncture insertion, and the conical tip did not produce any deflection that would couple with the deflection arising due to active needle actuation. We modified the surface of the needle shaft that interacted with the tissue to reduce the friction force as a measure of reducing the needle insertion force. Several studies have observed reduced insertion force with bioinspired needle design modifications [4]. The reduction in insertion force with a bioinspired passive needle has also been linked to decreased tissue deformation and tissue damage [6]. A mosquito proboscis-inspired biopsy needle design showed a reduction in insertion force and tissue deformation in tissue-mimicking gel [7]. Gidde et al. [8] performed experiments with a mosquito proboscis-inspired passive needle (a 3D printed needle of outer diameter of 3mm) prototype on tissue-mimicking gel and biological tissue and achieved a reduction in insertion force of 39%, tissue deformation reduction of 48%, and tissue damage reduction of 27%. Acharya et al. [9] modified the smooth cannula on an active needle to form a mosquito proboscis-inspired geometry. They also added vibration during insertion to improve the needle insertion mechanics and control.

In this study, we modified the active needle design initially proposed by Acharya et al. [10,11]. The adaptation involved incorporating a mosquito proboscis-inspired feature onto the needle cannula. The original design consisted of an active stylet, whose tip was deflected by a shape memory alloy (SMA) wire actuator and a compliant cannula. The outer surface of the cannula interacted with the tissue medium during insertion. We modified the outer surface of the cannula to accommodate a maxilla shape - a jagged structure found in mosquito proboscis, as shown in Fig. 1. The maxilla shape was scaled

up and applied to the needle cannula. The research involved measuring and comparing the mosquito proboscis-inspired active needle's insertion force, needle tip deflection, trajectory tracking error, and control effort against the active needle with the regular cannula.

Figure 1: Schematic of mosquito proboscis showing five components: labrum tip, pharynx, mandible, maxilla, and labium [8]

2. Materials and Methods

This segment is divided into three sections. The first focuses on designing and fabricating a mosquito proboscis-inspired cannula for percutaneous needles. The second section describes the experimental method used to evaluate the changes in needle insertion force and tip deflection during tissue insertion when utilizing the mosquito proboscis-inspired cannula compared to the conventional cannula. Lastly, the third section explains the impact of the mosquito proboscis-inspired cannula on control parameters such as trajectory tracking error and control effort in active needles.

2.1. Design and Fabrication of Mosquito Proboscis-inspired Cannula

A cannula tube inspired by a mosquito proboscis surface geometry was designed and manufactured for incorporating into the SMA-actuated needle. A 180 mm long mosquito proboscis-inspired cannula was fabricated by 3D printing the surface profile on a polymer sheet with dimensions inspired by Gidde et al. [6], such as maxilla angle (M_A) and maxilla spacing (t_h). The thin sheet of rubber-like polymer with a regular smooth surface and mosquito proboscis-inspired barbed surface profile was 3D printed (see Fig. 2(a)) with Elastico^{TM} material using a Stratasys J35 printer. Figure 2(b) shows the detailed parameter of the thin sheet's cross-section with maxilla angle (M_A) of 170°, length (L) of 180mm,

outer thickness (t_1) of 0.45mm, inner thickness (t_2) of 0.3mm, and maxilla spacing (t_h) of 0.2mm. The printed polymer sheets were rolled on top of thin polytetrafluoroethylene (PTFE) tube (outer diameter of 2.57mm) to create a regular smooth cannula and a mosquito proboscis-inspired barbed cannula (Fig. 2(c)). The final outer diameters of both cannulas were 3.5mm. The SMA-actuated active stylet with a conical tip and a distal bending region (Fig. 2(d)), developed by Acharya et al. [10], was inserted into the two types of cannula tubes.

Figure 2: (a) 3D printed polymer sheets with the mosquito proboscis-inspired jagged and the smooth surface, (b) cross-section geometry of the sheet with the parameters: maxilla angle (M_A) of 170°, length (L) of 180mm, outer thickness (t_1) of 0.45mm, inner thickness (t_2) of 0.3mm, and maxilla spacing (t_h) of 0.2mm, (c) polymer sheets rolled into cannula tubes (outer diameter: 3.5mm), (d) SMA-actuated needle stylet

2.2. Measuring Insertion Force and Deflection in Needles with Different Cannulas

The impacts of the mosquito proboscis-inspired cannula on conventional passive bevel tip needles and SMA-actuated active needles were investigated by measuring the insertion force and needle tip deflection. The insertion force combines cutting force at the needle tip and friction force on the needle shaft due to interaction with the tissue. The cutting force is considered constant, and friction force grows with insertion depth. During the insertion, the jagged shape in cannula reduces the needle tissue contact area compared to the smooth surface, resulting in a lower friction force, thus the lower insertion force [6,12]. A polyvinyl chloride (PVC) phantom tissue equivalent to 20kPa stiffness resembling prostate tissue was prepared for needle insertion experiments [3]. The needle was assembled into a robotic

needle insertion setup, as shown in Fig. 3. The needle insertion setup consisted of a linear stage unislide that inserted the needle into phantom tissue along the Z-direction. The needle was inserted up to 150mm insertion depth into the phantom tissue at a constant velocity of 1mm/s. First, the passive bevel tip needle with the regular cannula and mosquito proboscis-inspired cannula was inserted into the phantom tissue, and the resulting insertion force and needle tip deflection were measured. Then the SMA-actuated active needle with the two cannula designs was inserted into the phantom tissue. The active needle was initially inserted up to 50mm into the phantom tissue without any SMA actuation and stopped. This was followed by SMA heating to the temperature of 100°C for full actuation, followed by additional 100mm insertion with the fully actuated needle tip. A proportional-integral-derivative (PID) controller was designed to take the temperature feedback from the SMA wire actuator with a 0.0762mm (0.003-inch) type K thermocouple (Omega, Stanford, CT) and electrically heat the SMA wire with pulse width modulation (PWM) power to the desired temperature [3]. A six-axis force/torque transducer Nano 17® (ATI Industrial Automation, Apex, NC) was attached to the needle base and connected to a data acquisition system for measuring insertion force. The resulting needle insertion force data were obtained using LabVIEW software (National Instruments (NI) Corporation, Austin, TX). The needle tip deflection was measured at the end of 150mm insertion depth using a scaled paper under the transparent phantom tissue. The results and discussion section presents the insertion force and needle tip deflection results for both types of cannulas in passive and active needles.

Figure 3: Robotic needle insertion test setup including linear stage, force sensor, NI data acquisition system, phantom tissue, and active needle with the SMA wire, thermocouple, and position sensor

2.3. Trajectory Tracking Control in Active Needle with Different Cannulas

The trajectory tracking control of the active needle with the regular cannula and that with the mosquito proboscis-inspired cannula was performed inside the phantom tissue, and a comparison of trajectory tracking error and control effort was made. The position (x, y, z) in the three-dimensional cartesian coordinate space was acquired as feedback using an electromagnetic (EM) position sensor (NDI, Canada) attached to the tip of the needle. The position feedback was used to actuate the SMA wire to desired strain such that desired planar needle tip deflection was obtained during tissue insertion. The active needle was initially inserted up to 50mm depth along Z-axis without SMA wire actuation and stopped (please refer to Fig. 3 for axis orientation). The needle did not deflect since the tip of the needle was conical-shaped and produced symmetrical cutting forces at the tip. For deflection tracking control in PVC phantom tissue, the active needle insertion from 50mm to 100mm insertion depth was performed at a velocity of 1mm/s, and the needle tip deflection reference trajectory along X-axis was created as setpoint $SP_x(t)$. The position sensor measured the process variable $PV_x(t)$ as the time series position data of the needle tip along the X-axis as represented by Eq. (1).

$$PV_x(t) = \sqrt{(x(t) - x(0))^2} \quad (1)$$

The error $e_x(t)$ along the X-axis at each instant of time was calculated as the difference between the desired position $SP_x(t)$ and $PV_x(t)$ of the needle tip deflection, as shown by Eq. (2).

$$e_x(t) = SP_x(t) - PV_x(t) \quad (2)$$

A proportional-integral (PI) controller was programmed using LabVIEW to actuate the needle tip deflection $x(t)$ perpendicular to the insertion direction. The PI loop time was set to 0.1sec such that at each loop, a new data point of the deflection trajectory was applied as the setpoint $SP_x(t)$. The error $e_x(t)$ was fed into the PI controller to obtain control effort $u_x(t)$, as shown in Eq. (3). $u_x(t)$ was measured in duty cycle (0% to 100%) of PWM power supplied to the SMA actuator in the needle. The controller gain K_c and integral time constant τ_i were manually tuned parameters and were kept constants for all experiments.

$$u_x(t) = K_c e_x(t) + \frac{K_c}{\tau_i} \int_0^t e_x(t)\, dt \quad (3)$$

The needle deflection tracking performance was evaluated by measuring root mean square error (RMSE) using Eq. (4).

$$RMSE = \sqrt{\frac{1}{n} \sum_i (e_{x_i})^2} \quad (4)$$

3. Results and Discussion

Figure 4 shows the effect of the mosquito proboscis-inspired cannula in both passive and active needles in terms of insertion force. The mosquito proboscis-inspired cannula reduced the insertion force in the passive bevel tip needle throughout the insertion into phantom tissue. At 150mm depth in phantom tissue, the insertion force in the passive

needle reduced from 7.78N to 6.95N (a 10.67% reduction) due to the modified cannula. The reduction in insertion force can be attributed to the reduction in frictional force between the modified cannula and the phantom tissue interface [8,9]. Similarly, the insertion force for the first 50mm insertion depth in the active needle was lower than the passive needle for both types of cannulas because the active needle did not deflect due to a conical tip. However, upon SMA actuation to 100°C, the active needle deflection increased during 50mm to 150mm insertion depth to a larger value than the passive needles. This caused the rapid increase in insertion force, surpassing the value of passive needles (after 90mm insertion depth, as shown by the red curve crossing the yellow curve in Fig. 4).

Figure 4: Insertion force measured at the needle base during insertion into phantom tissue

Similarly, tip deflection achieved at 150mm insertion depth inside phantom tissue is presented in Fig. 5. The mosquito proboscis-inspired cannula increased the tip deflection of the passive needle from 10.48mm to 14.68mm, which is a 40.10% increment. The tip deflection increased from 26.88mm to 30.35mm (a 12.91% increment) for active needles by modifying the cannula. Therefore, the mosquito proboscis-inspired cannula enabled higher tip deflection, which is desirable for needle steering.

Figure 5: Needle tip deflection at 150mm insertion depth in phantom tissue

Investigating the mechanics and control of the mosquito proboscis-inspired cannula for active steerable needle insertion into PVC phantom tissue yielded promising results. The insertion force was reduced, and the needle tip deflection was increased, improving the needle steering feature. With the proposed cannula, the SMA-actuated active needle achieved a larger deflection for an equal amount of SMA actuator heating (temperature of 100°C), meaning that lesser energy would be required to achieve equal deflection. Therefore, the increased deflection would also improve the control performance in trajectory tracking of the needle inside the tissue. The active needles with two different cannulas were inserted into the phantom tissue to follow a reference deflection trajectory. The insertion speed was kept constant at 1mm/s, but the deflection of the needle tip was controlled using a PI controller with needle tip position feedback. The result of the SMA-actuated needle tip deflection tracking inside the phantom tissue is shown in Fig. 6. The RMSE of deflection tracking for the needle with mosquito proboscis-inspired cannula was measured to be 0.44mm, and that with regular cannula was measured to be 0.72mm. Similarly, the average control duty cycle from the PI controller for actuating deflection along the reference path for the active needle was 51.00% for the regular cannula and 42.00% for the mosquito proboscis-inspired cannula. The reduction in tracking error and control effort shows that the mosquito-proboscis inspired cannula helped improve the needle insertion mechanics which lead to improvement in control parameters.

Figure 6: Active needle tip deflection tracking in phantom tissue for different cannulas

4. Conclusions

In this study, a bioinspired cannula inspired by the mosquito proboscis was developed and created specifically for SMA-actuated active needles. The focus of the research was to investigate the impact of this new cannula on the mechanics and control of active needles. The results revealed noteworthy changes. The mosquito proboscis-inspired cannula on the passive bevel tip needle demonstrated a 10.67% reduction in insertion force. Similarly, the insertion force for the active needle decreased initially for smaller depths but increased at greater depths due to increased tip deflection. The tip deflection in the active needle increased by 12.91% at 150mm insertion depth for the equal amount of SMA actuation when the cannula was modified. The enhanced performance of the mosquito proboscis-inspired cannula was further evident in active needle tracking, as it significantly reduced the root mean square error (RMSE) by 39.00% and improved the control effort by lowering the duty cycle by 17.65%. These promising outcomes signify the potential of the proposed bioinspired cannula to enhance needle steering accuracy and ease control efforts in the active needles. The future scope of this research extends to testing the active needle with the mosquito proboscis-inspired cannula in diverse biological tissues, aiming to explore the benefits and applicability in clinical settings. Additionally, a comprehensive histology study will be conducted to evaluate tissue damage, which is essential for assessing the effectiveness and safety of this innovative approach in clinical applications.

Conflict of Interest Statement

The authors declare no conflict of interest.

Acknowledgment

The authors would like to acknowledge the National Science Foundation (CMMI Award #1917711) for the financial support.

Nomenclature

t	Time, s
$PV_x(t)$	Process variable deflection along x-axis, mm
$SP_x(t)$	Set point deflection along x-axis, mm
e_x(t)	Error between actual and reference needle tip deflection, mm
K_c	Controller gain
τ_i	Integral time constant

References

[1] Podder, T. K., Dicker, A. P., Hutapea, P., Darvish, K., and Yu, Y., 2012, "A novel curvilinear approach for prostate seed implantation," Med. Phys., vol. 39, no. 4, pp. 1887–1892, doi: 10.1118/1.3694110

[2] Leibinger, A., Oldfield, M. J., and Rodriguez y Baena, F., 2016, "Minimally disruptive needle insertion: a biologically inspired solution," Interface focus, 6(3), 20150107, doi: 10.1098/rsfs.2015.0107

[3] Acharya S. R., Hutapea P. "Design and evaluation of shape memory alloy-actuated active needle using finite element analysis and deflection tracking control in soft tissues," Int J Med Robot. 2023;e2554, doi: 10.1002/rcs.2554

[4] Ma, Y., Xiao, X., Ren, H., and Meng, M. Q. H., 2022, "A review of bio-inspired needle for percutaneous interventions," Biomimetic Intelligence and Robotics, 2(4), 100064, doi:10.1016/j.birob.2022.100064.

[5] Simone, C., and Okamura, A. M., 2022, "Modeling of needle insertion forces for robot-assisted percutaneous therapy," In Proceedings 2002 IEEE International Conference on Robotics and Automation (Cat. No. 02CH37292), 2, pp. 2085-2091, doi: 10.1109/ROBOT.2002.1014848.

[6] Gidde, S. T. R., Acharya, S. R., Kandel, S., Pleshko, N., and Hutapea, P., 2022, "Assessment of tissue damage from mosquito proboscis-inspired surgical needle," Minimally Invasive Therapy & Allied Technologies, 31(7), pp. 1112-1121, doi: 10.1080/13645706.2022.2051718.

[7] Li, D. R. A., Putra, B. K., Chen, L., Montgometry S. J., and Shih, A., 2020, "Mosquito proboscis-inspired needle insertion to reduce tissue deformation and

organ displacement," Scientific Reports, 10, 12248, doi: 10.1038/s41598-020-68596-w.

[8] Gidde, S. T. R., Islam, S., Kim, A., and Hutapea, P., 2023, "Experimental study of mosquito proboscis-inspired needle to minimize insertion force and tissue deformation," Proceedings of the Institution of Mechanical Engineers, Part H: Journal of Engineering in Medicine, 237(1), pp. 113-123, doi: 10.1177/09544119221137133.

[9] Acharya S. R., and Hutapea, P., 2023, "An experimental study on the mechanics and control of SMA-actuated bioinspired needle," Bioinspiration & Biomimetics (under review) https://iopscience.iop.org/journal/1748-3190

[10] Acharya, S. R., and Hutapea, P., 2021, "Towards clinically-relevant shape memory alloy actuated active steerable needle," Proceedings of the ASME 2021 Conference on Smart Materials, Adaptive Structures and Intelligent Systems, V001T05A020, doi: 10.1115/smasis2021-68409.

[11] Acharya, S. R., and Hutapea, P., 2022, "Design and control strategy of tip manipulation for shape memory alloy actuated steerable needle," Proceedings of the ASME 2022 Conference on Smart Materials, Adaptive Structures and Intelligent Systems, V001T04A011, doi: 10.1115/smasis2022-91002.

[12] Izumi, H., Yajima, T., Aoyagi, S., Tagaqa, N., Arai, Y., Hirata, M., and Yorifuji, S., 2008, "Combined harpoonlike jagged microneedles imitating mosquito's proboscis and its insertion experiment with vibration," IEEJ Transactions on Electrical and Electronic Engineering, 3(4), pp. 425-431, doi:10.1002/tee.20295.

Figure Captions List

Figure 1: Schematic of mosquito proboscis showing five components: labrum tip, pharynx, mandible, maxilla, and labium [8]

Figure 2: (a) 3D printed polymer sheets with the mosquito proboscis-inspired jagged and the smooth surface, (b) cross-section geometry of the sheet with the parameters: maxilla angle (M_A) of 170°, length (L) of 180mm, outer thickness (t_1) of 0.45mm, inner thickness (t_2) of 0.3mm, and maxilla spacing (t_h) of 0.2mm, (c) polymer sheets rolled into cannula tubes (outer diameter: 3.5mm), (d) SMA-actuated needle stylet

Figure 3: Robotic needle insertion test setup including linear stage, force sensor, NI data acquisition system, phantom tissue, and active needle with the SMA wire, thermocouple, and position sensor

Figure 4: Insertion force measured at the needle base during insertion into phantom tissue

Figure 5: Needle tip deflection at 150mm insertion depth in phantom tissue

Figure 6: Active needle tip deflection tracking in phantom tissue for different cannulas

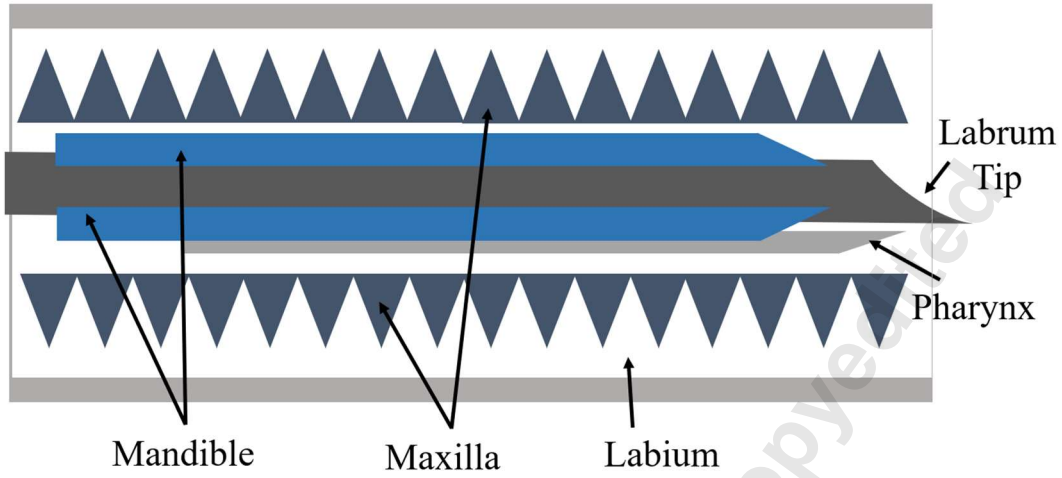

Figure 1: Schematic of mosquito proboscis showing five components: labrum tip, pharynx, mandible, maxilla, and labium [8]

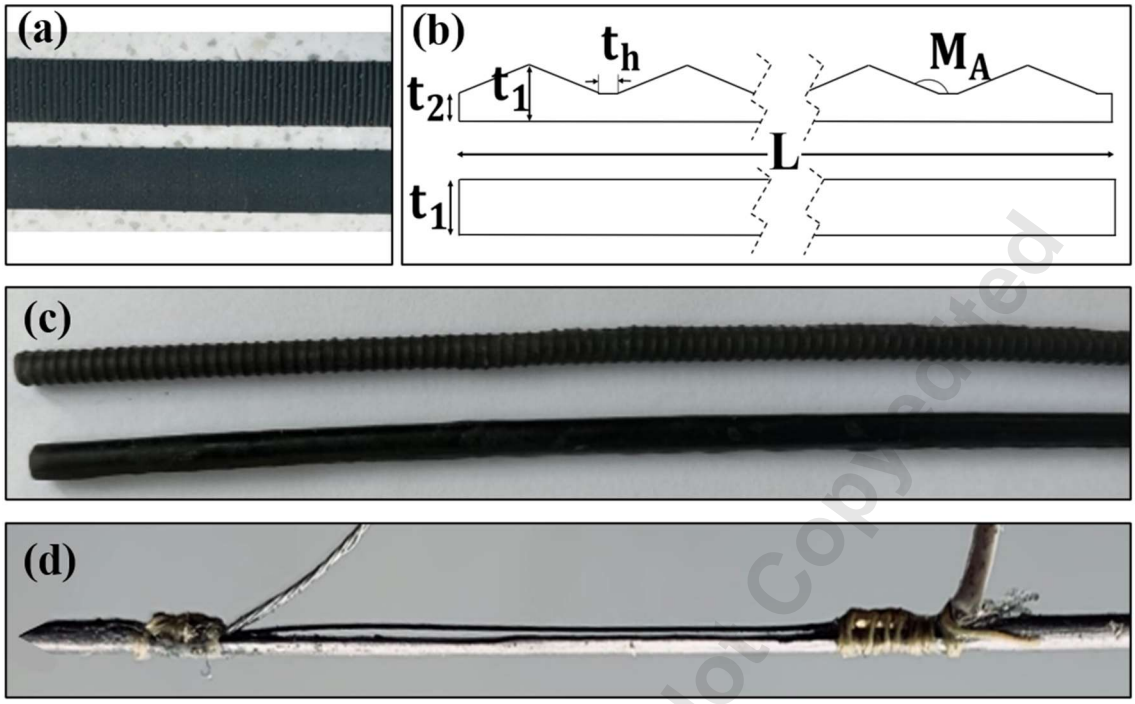

Figure 2: (a) 3D printed polymer sheets with the mosquito proboscis-inspired jagged and the smooth surface, (b) cross-section geometry of the sheet with the parameters: maxilla angle (M_A) of 170°, length (L) of 180mm, outer thickness (t_1) of 0.45mm, inner thickness (t_2) of 0.3mm, and maxilla spacing (t_h) of 0.2mm, (c) polymer sheets rolled into cannula tubes (outer diameter: 3.5mm), (d) SMA-actuated needle stylet

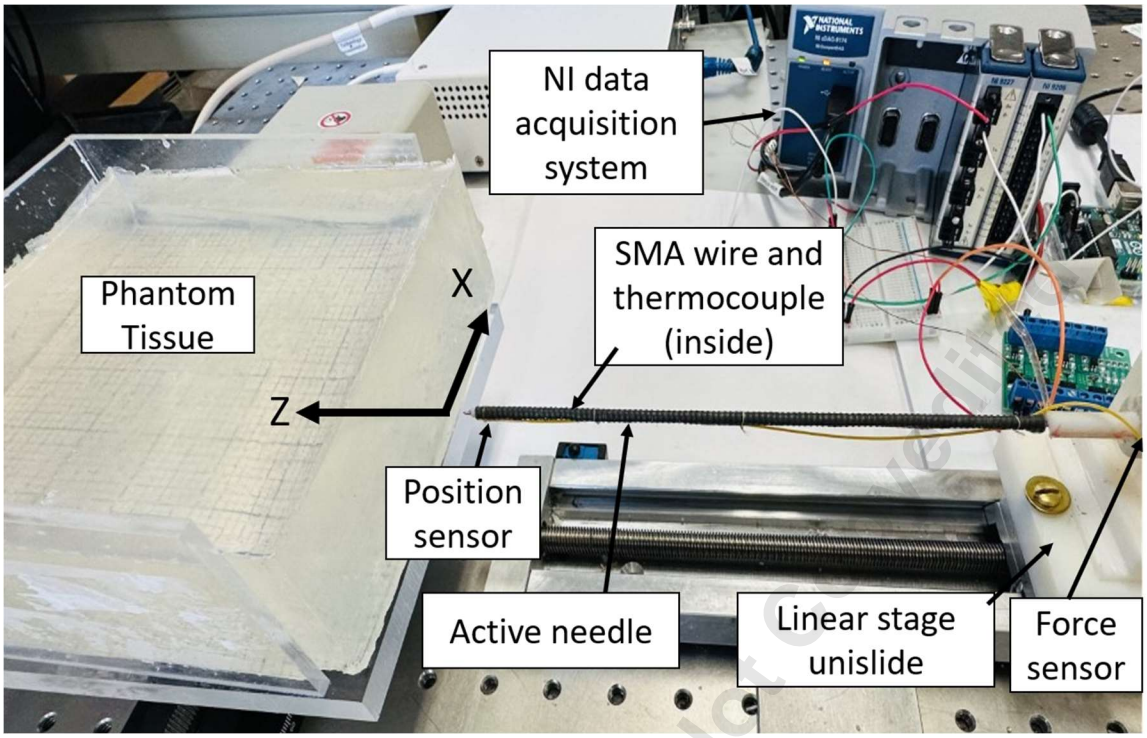

Figure 3: Robotic needle insertion test setup including linear stage, force sensor, NI data acquisition system, phantom tissue, and active needle with the SMA wire, thermocouple, and position sensor

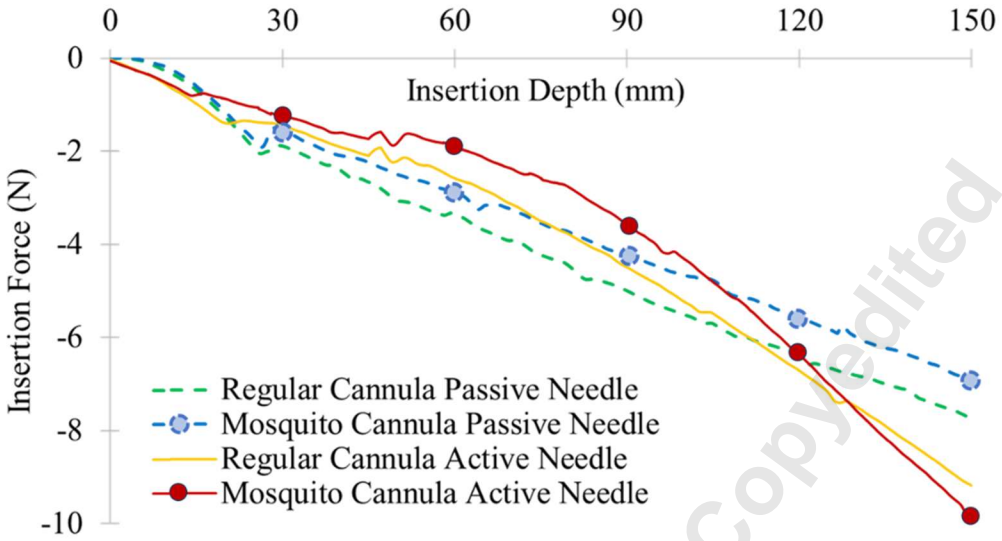

Figure 4: Insertion force measured at the needle base during insertion into phantom tissue

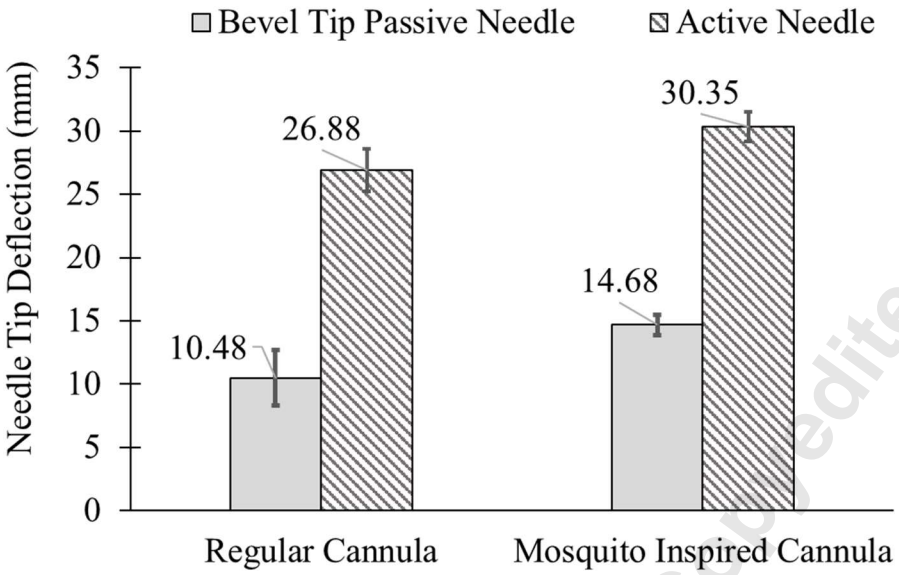

Figure 5: Needle tip deflection at 150mm insertion depth in phantom tissue

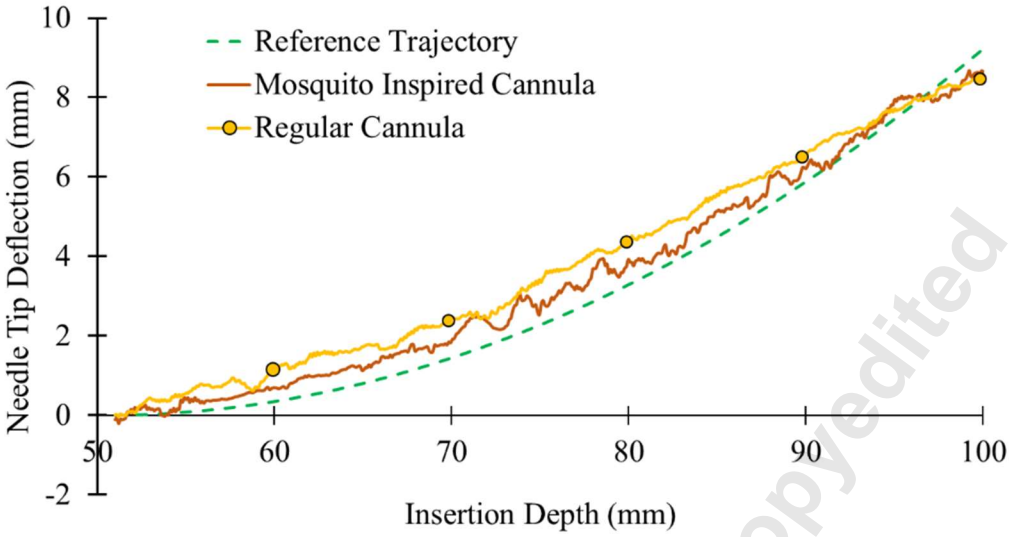

Figure 6: Active needle tip deflection tracking in phantom tissue for different cannulas